Nucleic Acid Nanostructures for Chemical and Biological Sensing

Arun Richard Chandrasekaran, Heitham Wady, and Hari K. K. Subramanian**

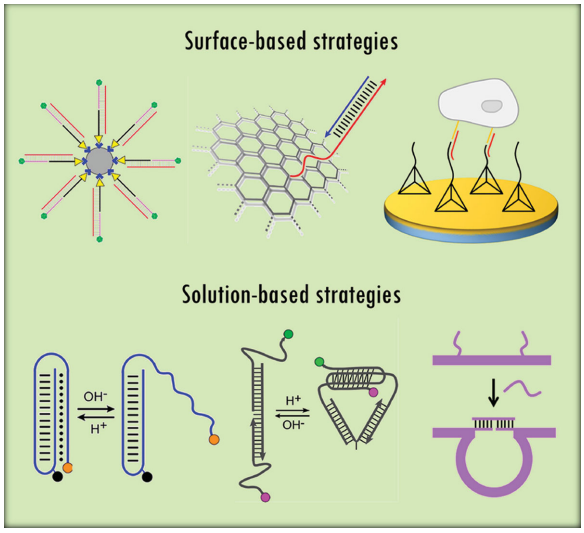

From the Contents

The nanoscale features of DNA have made it a useful molecule for bottom-up construction of nanomaterials, for example, two- and three-dimensional lattices, nanomachines, and nanodevices. One of the emerging applications of such DNA-based nanostructures is in chemical and biological sensing, where they have proven to be cost-effective, sensitive and have shown promise as point-of-care diagnostic tools. DNA is an ideal molecule for sensing not only because of its specificity but also because it is robust and can function under a broad range of biologically relevant temperatures and conditions. DNA nanostructure-based sensors provide biocompatibility and highly specific detection based on the molecular recognition properties of DNA. They can be used for the detection of single nucleotide polymorphism and to sense pH both in solution and in cells. They have also been used to detect clinically relevant tumor biomarkers. In this review, recent advances in DNA-based biosensors for pH, nucleic acids, tumor biomarkers and cancer cell detection are introduced. Some challenges that lie ahead for such biosensors to effectively compete with established technologies are also discussed.

1. Introduction

Nanotechnology has opened up new avenues for a wide variety of applications ranging from biomaterials for tissue engineering[1] to protection against toxic agents.[2] The nanomaterials used for these applications are prepared by either the top-down or the bottom-up approach. Biomolecules, especially DNA, has been successfully used for bottom-up construction of nanomaterials.[3] The main features of DNA — its inherent nanoscale dimensions and specific molecular recognition — make it a versatile nanoscale building block. Researchers have taken advantage of this to construct two-[4] and three-dimensional lattices,[5] topologically-linked arrays,[6] nanomachines[7] and nanodevices.[8] The occurrence of different conformations of DNA[9] depending on the ionic environment has also been used to construct devices based on conformational changes.[10] DNA as a material has shown promise in applications related to nanoelectronics,[11] biomolecular computations,[12] cellular imaging[13] and drug delivery.[14] One other emerging application is in chemical and biological sensing, where DNA-based biosensors have proven to be cost-effective, sensitive and have the potential to be used as point-of-care diagnostic tools. With the aid of a 'toolkit' of enzymes, DNA-based nanostructures can be used for sensitive, multiplexed detection strategies.[15] DNA is a desirable molecule for sensing not only because of its specificity but also because of its robustness and ability to function under a wide range of biologically relevant temperatures and conditions.[16] In this review we introduce recent advances in DNA-based biosensors for pH detection, nucleic acids, tumor biomarkers and cancer cell detection (**Figure 1**) and discuss the opportunities and challenges that lie ahead for such sensors.

2. Nucleic Acids Detection and Genotyping

Genotyping of human diseases depends largely on specific molecular detection of nucleic acids or proteins. Strategies based on microarrays,[17] reverse transcription polymerase chain reaction (RT-PCR),[18] and the next-generation sequencing technology[19] are convenient for high-throughput processing. However, they are still expensive,[20] require probe labeling, and detection of biological samples at very low concentrations is still difficult.[21] The advent of biocompatible DNA nanostructures has provided highly specific and sensitive detection based on the molecular recognition properties of DNA.

Biosensors based on DNA nanostructures often utilize key components of traditional sensing methods such as the use of a fluorescent signal probe.[22] In such cases, the output signal can be amplified by strand displacement polymerization reaction (**Figure 2**a). However, such methods also involve multiple steps for detection and amplification. For example, Guo et al.[22] used a molecular beacon as their reporter. The loop region of the beacon is designed to be complementary to the target sequence. On target binding, the hairpin is open thus causing a fluorescent signal. This signal is further amplified by polymerase strand displacement thus recycling the target to enhance the signal.

DNA tetrahedra[23] are a class of nanostructures that exhibit structural rigidity and provide spatial positioning of functional guests on their edges and/or vertices. Taking advantage of this, Pei et al.[24] have created DNA tetrahedron-based electrochemical biosensors by combining them with surface-based assays (Figure 2b). They bound the bottom three vertices of the tetrahedral DNA probe to a gold electrode surface via thiol modifications. The fourth vertex was designed to contain a single-stranded DNA (ssDNA) probe that points outward from the surface and is complementary to part of the target. In surface-based assays, target molecules have reduced access to probes compared to probe-target recognition in solution.[25] However, the strategy used by Pei et al. [24] allows control over positioning of the probes away from the surface (depending on the dimensions of the tetrahedra), thereby providing enhanced accessibility of the probes compared to linear or stem-loop probe structures.[26] When part of the target binds to the probe, a biotinylated reporter probe binds to the remaining part of the target. This hybridization event is then transduced into electrochemical signals through the specific binding of an avidin-HRP (horseradish peroxidase) conjugate to the biotin, leading to enzyme turnover-based signal transduction.[27] Specifically, the tetrahedral structure used in this study contained DNA probes with well-defined probe-to-probe spacing of ~4 nm with a surface density estimate of 4.8×10^{12} tetrahedral probes per cm^2. The lateral spacing and interactions of these tetrahedral nanostructures can be controlled by altering the size of the tetrahedra, leading to decreased hybridization times and increased hybridization efficiency.[28] This is important as control over the packing density of probes on the surface and its conformation are known to play a critical role in the efficiency of target detection.[29] Moreover, this electrochemical sensor showed significant signal differences for a single base pair mismatch between the target and the probe DNA.

Analysis of biomolecular interactions can be realized using DNA nanoswitches.[30] Chandrasekaran et al.[31] used this strategy for the detection of specific target nucleic acid sequences. Target binding causes the switch to undergo a conformational change from its linear 'off' state to a looped 'on' state. Detection of the target was done using a simple

Dr. A. R. Chandrasekaran[+]
The RNA Institute
University at Albany
State University of New York
Albany, NY 12203, USA
E-mail: arunrichard@nyu.edu
H. Wady[+]
Upstate Medical University
State University of New York
Syracuse, NY 13210, USA
Dr. H. K. K. Subramanian
Department of Mechanical Engineering
University of California
Riverside, CA 92521, USA
E-mail: harikks@engr.ucr.edu
[+]A. R. Chandrasekaran and H. Wady contributed equally to this manuscript.

DOI: 10.1002/smll.201503854

gel electrophoresis read-out (Figure 2c). Such programmable switches with an easy read-out have the potential to detect nucleic acid markers that are of biological relevance and will be useful for point-of-care diagnostics. Lateral flow nucleic acid biosensors[32] have also been developed for detecting nucleic acid sequences. These sensors utilize isothermal strand-displacement polymerase reaction[22] and gold nanoparticles (AuNPs) to provide a visual read-out. The signal amplification process is similar to that described in Figure 2a. This biosensor works based on the conformational change of a DNA probe upon target binding and can be read-out as a color change that happens due to aggregation of the AuNPs (Figure 2d). This method also allowed for quantitative detection by analyzing the optical density of the test line.

DNA origami[33] has been applied to construct useful devices such as a molecular analog of DNA microarray chips. Ke et al.[34] inserted single-stranded DNA probes (complementary to the target nucleic acid) at precise positions of an origami tile. Hybridization of the probe tiles to the target in solution was detected using atomic force microscopy (AFM) (Figure 2e) based on the difference in elastic properties of single-stranded (probes without target) and double-stranded DNA (probes bound to target). The other advantage of this strategy is that the origami structure can be designed to control the inter-probe distance.

Single nucleotide polymorphisms (SNPs) are the most common genetic variation in the human genome.[35] DNA nanostructrues have recently been developed for highly specific detection of SNPs.[36] Chen et al.[37] reported one such example based on conditionally fluorescent molecular probes (**Figure 3**a). This strategy was based on double-stranded toe-hold exchange and involved a double-stranded probe with forked single-stranded overhangs, one containing a fluorophore and the other containing a quencher. Binding of a proper target initiates toe-hold strand exchange and causes separation of the fluorophore from the quencher, thus increasing fluorescence. However, a target with even a single mismatch has a much lower binding affinity causing the formation of a duplex with two mismatch bubbles. Tetrahedral DNA nanostructure-based electrochemical sensors have also been used for SNP detection (Figure 3b).[24] The discrimination factors between a properly matched target (A:T) and single-nucleotide mismatched targets (T:T, C:T, G:T) were found to be 150, 1000, and 10000, respectively. These biosensors provide a sensitive detection route for SNPs compared to ssDNA probe-based methods.

DNA origami platforms have also been used to provide a visual read-out of SNPs. Zhang et al.[38] used a DNA origami-based strategy for label-free SNP detection in homogeneous solutions based on previously designed DNA origami chips[39] and enhanced its specificity by incorporating a toehold-mediated strand-displacement[40] reaction. They used an asymmetric, map-shaped DNA origami chip that was designed to contain a line of protruding ssDNA capture probes, which were hybridized with biotinylated, partially complementary reporter probes (Figure 3c) that can recruit streptavidin. In the presence of a target that is perfectly complementary to the capture probe, the toehold region is first hybridized followed by branch migration, eventually resulting in complete displacement of the reporter probe. Thus, the streptavidin, seen as white bulges in AFM images is displaced from the origami in the presence of a perfectly complementary target DNA but not in the presence of a sequence with even a single mismatch.

It is known that nucleotide mismatches drastically slow down the progression of branch migration beyond a single mismatch site.[41] Subramanian et al.[42] used this strategy to produce a direct visual readout of the target nucleotide contained in the probe sequence using an AFM (Figure 3d). They designed an origami platform containing graphical representations of A, T, G, and C, the four possible nucleotide alphabetic characters. The symbol containing the test nucleotide identity disappears in the presence of the probe. They used this method to study SNPs and also demonstrated the feasibility of using this approach for a heterozygous probe, making it more relevant to genomes of diploid organisms. **Table 1** compares the different techniques for nucleic acid detection discussed in this section.

Arun Richard Chandrasekaran graduated with a PhD in Chemistry in 2015 from New York University, where he conducted research under the supervision of Prof. Nadrian Seeman. He is currently a Post-doctoral Research Associate at The RNA Institute, University at Albany, State University of New York. His research interests include the design, construction, and characterization of DNA nanostructures. He is currently working on developing programmable DNA nanoswitches for the detection of nucleic acid biomarkers.

Heitham Wady received his B.S. in Chemistry from the New York University in 2013. He then worked as a Research Assistant under Dr. Neil Schluger at Columbia University, USA. In 2014, he was accepted into and matriculated to SUNY Upstate Medical University, USA, as a medical student. His research interests include DNA nanotechnology, cancer genome sequencing, and protein modeling.

Hari K. K. Subramanian received his Ph.D. in Chemistry from the New York University in 2011. He then worked as a postdoctoral researcher with Prof. Thomas D. Tullius at Boston University, USA. In 2013, he joined Prof. Elisa Franco's laboratory at University of California – Riverside, USA, as a postdoctoral researcher. His research interests include DNA nanotechnology, RNA nanotechnology, dynamic nucleic acid circuits and oxidative damage of genomic DNA.

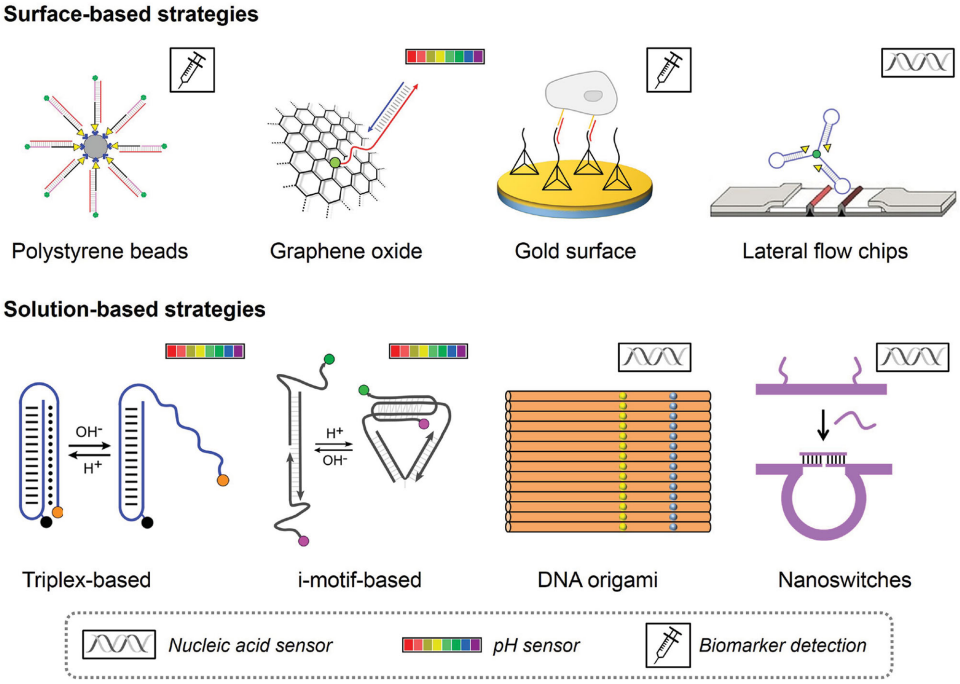

Figure 1. Strategies for chemical and biological sensing using nucleic acid nanostructures. Illustration showing the detection of biomarkers, nucleic acids, and pH levels by various DNA-based nanostructures. These strategies can be either surface-based (top row) or solution-based (bottom row). Lateral flow chips adapted with permission.[32] Copyright 2012, RSC.

3. Biomarker Detection

One of the biggest challenges in clinical diagnostics lies with the ability of immunological assays to detect reliably, with precision and specificity, the biomarkers for a variety of diseases.[43] Detection of ultralow concentrations of nucleic acid biomarkers in a complex cellular environment can be quite difficult. Thus, enhanced biomarker detection methods have gained considerable attention recently due to their potential applications in early diagnosis of infections.[44]

Li et al.[45] used the multivalent and anisotropic properties of dendrimer-like DNA (DL-DNA)[46] to create multicolor fluorescence-intensity encoded DNA barcodes with attached molecular probes. Polystyrene microbeads were utilized to amplify the fluorescent signals (**Figure 4**a). Hybridization of the barcodes to different targets produced specific colors on the membrane that can be later identified using a preassigned decoding library. These nanobarcodes provided multiplexed identification along with a rapid and sensitive detection of DNA from three pathogenic species: *B. anthracis*, Ebola, and SARS.

Electrochemical techniques, being convenient and affordable, are particularly alluring for DNA detection.[47] However, sensitivity is a critical limiting variable of electrochemical DNA biosensors. To address this problem, Chen et al.[48] used long-range self-assembled DNA constructs that act as scaffolds for signal magnification. They used this system for detecting Human Immunodeficiency Virus (HIV) DNA. Two auxiliary probes were designed to trigger a series of hybridizations leading to long-range self-assembly of micrometer-long DNA nanostructures. The fragment of the 3′ end of one of these probes was designed to bind to the target DNA (a 38-nucleotide sequence from the human immunodeficiency virus). Hexaammineruthenium (III) chloride (RuHex) then bound to the negatively charged phosphate backbone of the DNA via electrostatic forces. The accumulation of RuHex to the electrode was read out as electrochemical output signals.

Early detection of cancer cells is paramount in clinical practice, often dictating cancer treatments and health outcomes, but can be difficult due to the low levels of circulating tumor cells in the peripheral blood.[49] Thus, a highly specific and sensitive detection method is needed. Zhou et al.[50] used multibranched hybridization chain reaction (mHCR) products with multiple biotins and branch points bound on DNA nanostructured gold electrode surfaces for cancer cell detection (Figure 4b). An antibody or an aptamer that binds to the epithelial cell adhesion molecule (EpCAM) is commonly used to catch the malignant cells.[51] In this study, a DNA probe was conjugated with a biotin-labeled EpCAM aptamer. On incubation of cancer cells with L-aptamers and avidin-HRP, the cancer cells were captured by the capturing probe on a DNA tetrahedron biosensor[24] attached to a gold electrode. This method provided a read-out signal for as low as 24 cancer cells. However, for cancer cell detection to be useful in clinical diagnostics, the threshold of detection should be five cancer cells or lower for predicting survival outcomes and metastasis.[52] To improve sensitivity, Zhou et al.[50] used the mHCR reaction to produce lengthy products with many biotins to amplify the signal and many branch points to create multivalent surface binding. This dual-functional mHCR allowed for signal amplification and multivalent binding, resulting in the synthesis of a DNA biosensor that could sensitively detect as few as four cancer cells, thus making the strategy clinically relevant.

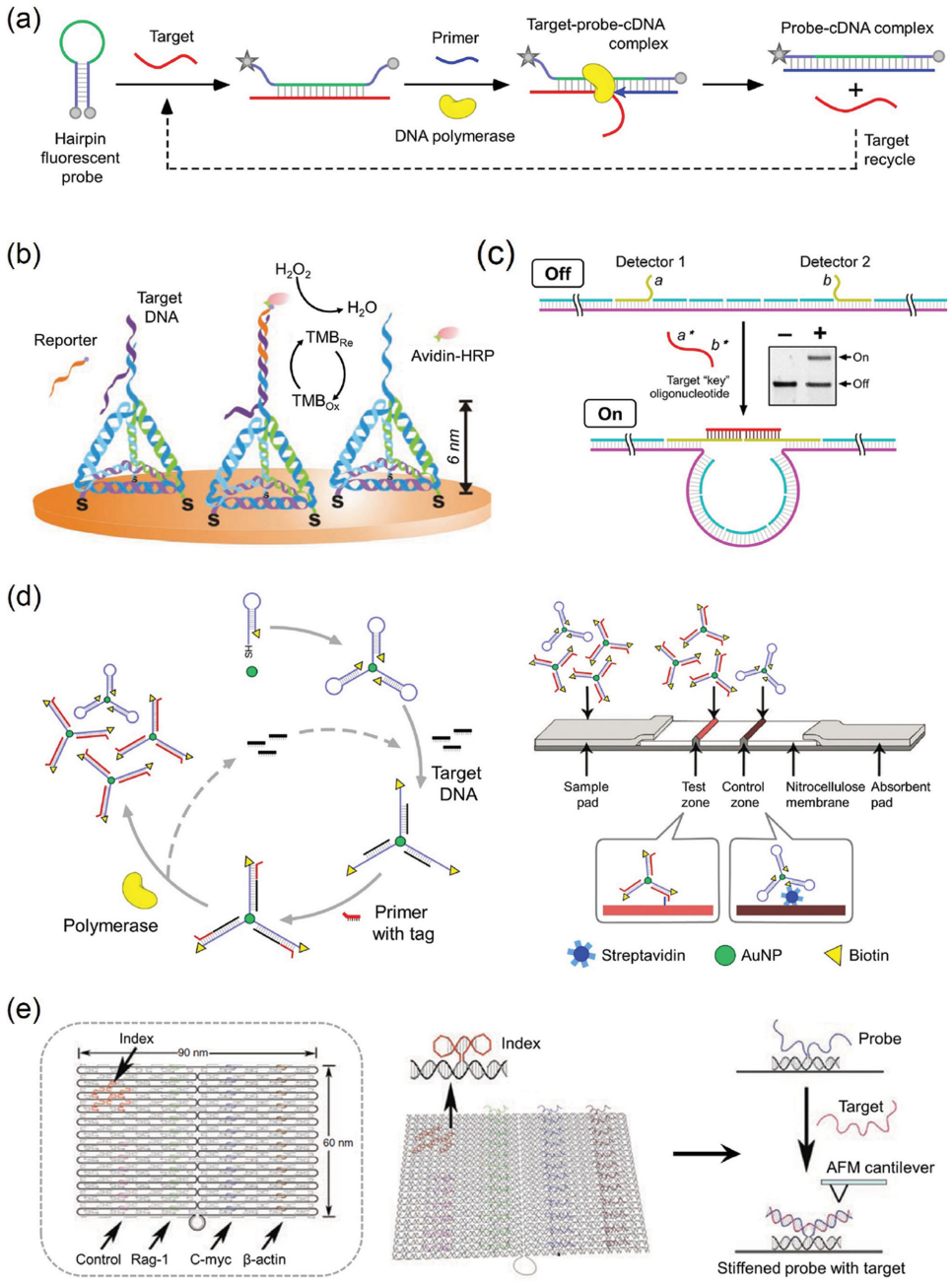

Figure 2. Strategies for nucleic acid sensing. a) Detection and amplification based on isothermal strand-displacement polymerization reaction. Adapted with permission.[22] Copyright 2009, Oxford University Press. b) DNA tetrahedron-based electrochemical sensor. Target binding event is transduced to electrochemical signal by the binding of an avidin-HRP conjugate to the biotin-tagged reporter probe. Adapted with permission.[24] c) Nanoswitch-based detection of target DNA sequences. Target binding induces a conformational change from a linear to a looped state which can be read out using gel electrophoresis (inset). Adapted with permission.[31] Copyright 2016, ACS. d) The cyclic pathway of sequence-tagged DNA complexes based on isothermal strand-displacement polymerization reaction (left) and its optical read-out based on a lateral flow biosensor (right). Adapted with permission.[32] Copyright 2012, RSC. e) *Left.* Schematic of the nucleic acid probe tiles with three different probes and a control probe. *Middle.* Molecular model of the tile with probes shown. *Right.* Target hybridization leads to the formation of an RNA-DNA duplex, and the stiffer V-shaped junction is detected using an AFM. Adapted with permission.[34] Copyright 2008, AAAS.

As discussed earlier in this review, DNA tetrahedra-based electrochemical biosensors immobilized on gold surfaces provide highly selective DNA detection capabilities.[24] Pei et al.[53] combined this strategy with DNA-bridged antibody immobilization[54] to create a highly functional immunological sensor (Figure 4c). The tetrahedral structure was similar to the one previously discussed[24] and contained a pendant "bridge DNA" on one vertex, and was immobilized onto a gold surface. The bridge hybridized to a complementary strand modified with a carboxyl group. The carboxyl group-terminated surface was conjugated to an antibody for tumor necrosis factor alpha (TNF-α), creating an antibody anchored surface for tumor marker detection. Immunological reactions occurring at the DNA tetrahedron-plated electrodes in the

www.MaterialsViews.com

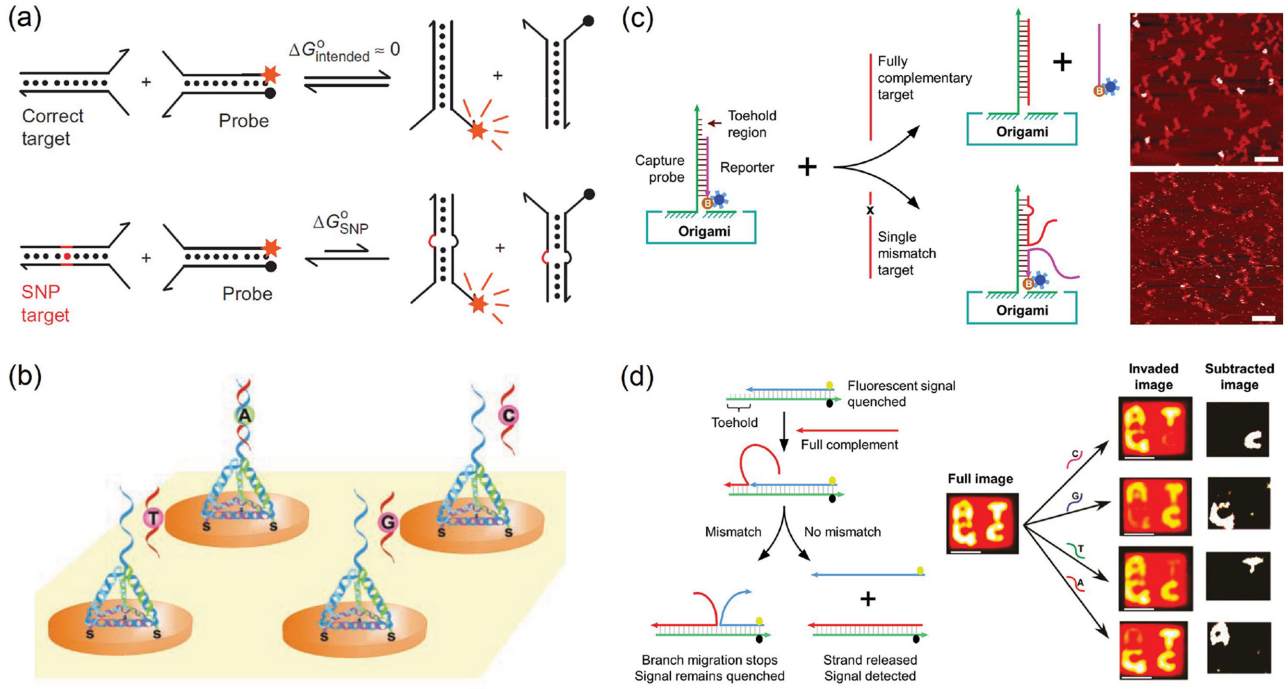

Figure 3. Detection of single nucleotide polymorphism. a) Conditionally fluorescent molecular probe based on double-stranded toehold exchange. Reproduced with permission.[37] Copyright 2013, NPG. b) DNA tetrahedron-based electrochemical read-out for SNP detection. Reproduced with permission.[24] c) A DNA origami-chip with toehold-mediated strand-displacement reaction for SNP detection. Scale bar: 250 nm. Adapted with permission.[38] d) An illustration of the branch-migration-based mismatch detection technique (left). AFM-based read-out of the nucleotide in the target probe (right). Scale bar: 50 nm. Adapted with permission.[42] Copyright 2011, ACS.

presence of TNF-α were read out as electrochemical signals through avidin-HRP interaction. This strategy provides a reusable sensing surface and more control over the orientation of antibodies on the surface making it more efficient for immunological sensing.

Recently, Ranallo et al. reported a DNA-based beacon for the detection of various antibodies and proteins.[55] They created a switch inspired by molecular beacons[56] that changes conformations on target binding. The switch was composed of a stem-loop system with two single stranded tails. The ends of these tails were modified to contain an appropriate target-specific recognition element. The stem region contains a fluorophore/quencher pair. Without the target, the stem remains closed and the fluorescent signal is quenched (Figure 4d). However, on target binding, the stem region is opened shifting the fluorophore away from the quencher thus causing a signal based on Fluorescence Resonance Energy Transfer (FRET). In the case of monovalent targets, binding of two targets to the two modified tails causes the stem to open because of steric hindrance between the targets. For bivalent targets, the stem opens due to distance-dependent binding of the recognition elements to two different locations on the target antibody. They used this sensor to detect a HIV biomarker anti-p17 antibody as well as other antibodies and protein targets. **Table 2** summarizes the functionalities of the sensors for biomarker detection discussed in this section.

Table 1. Summary of nucleic acid detection strategies.

Structure	Strategy	Read out	Target	LOD	Amplification	Reference
Stem-loop	Isothermal strand-displacement polymerization reaction	Fluorescence	ssDNA	6.4 fM	Yes	[22]
DNA tetrahedron/gold surface	TMB-based electrochemical transduction	Amperometry	Thrombin ssDNA	100 pM 1 pM	No	[24]
DNA nanoswitch	Conformational change	Gel electrophoresis	ssDNA	12.5 pM	No	[31]
DNA-AuNP conjugates	AuNP aggregation	Color change	Human genomic DNA	25 ng/ml	Yes	[32]
DNA origami/ssDNA probes	Elastic properties of ssDNA, dsDNA and DNA:RNA hybrids	AFM	ssRNA	200 pM	No	[34]
DNA origami/STV-biotin	Toehold mediated strand displacement/ biotin-STV	AFM	SNP detection	N/A	No	[38]
DNA origami/hairpins	Toehold mediated strand displacement	AFM	SNP detection	N/A	No	[42]

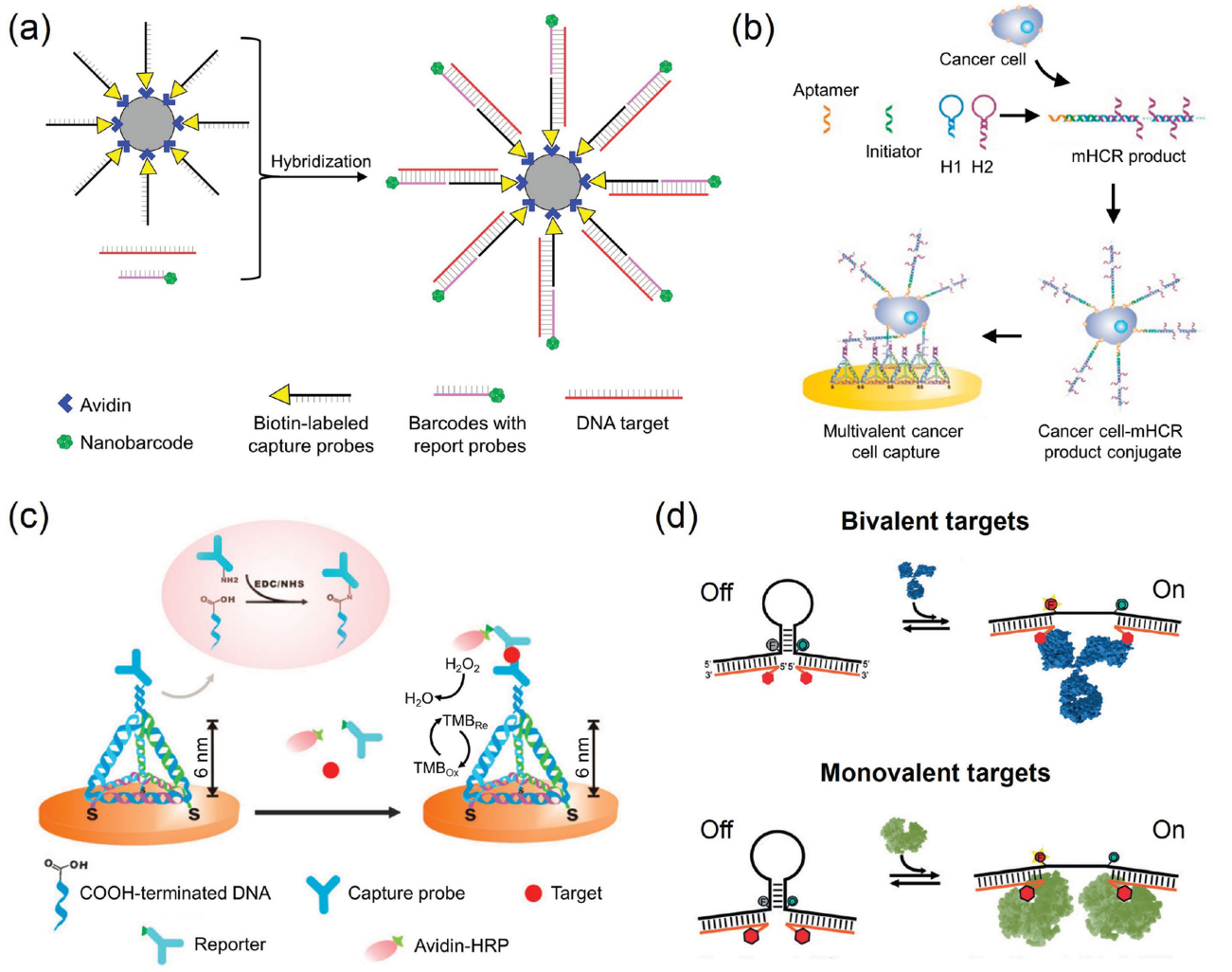

Figure 4. Biomarker detection using DNA nanostructures. a) Nanobarcodes for microbead-based DNA detection using fluorescence microscopy.[45] b) DNA-nanostructure-based multibranched HCR (mHCR) reaction to detect cancer cells. Adapted with permission.[50] Copyright 2014, ACS. c) DNA tetrahedron-based probes for electrochemical sensing of antibody immobilization. Adapted with permission.[53] Copyright 2011, RSC. d) DNA nanoswitch-based beacon for the detection of antibodies and proteins. Reproduced with permission.[55]

4. pH Sensing

The human body is composed of a plethora of complex systems working in a synchronized fashion to maintain optimal conditions necessary for life. There exists a physiological balance to maintain relatively stable and constant internal conditions. Acid-base homeostasis involves a tightly regulated process monitoring the pH of different cellular compartments, body fluids, and organs.[57] Natural pH sensors in the human body exist to regulate and balance pH

Table 2. Summary of biomarker detection strategies.

Structure	Strategy	Read out	Target	LOD	Amplification	Reference
DNA dendrimer-based barcodes	DNA hybridization	Fluorescence microscopy/dot blotting/flow cytometry	DNA from *B. anthracis*, Ebola, SARS	620 attomole	Yes	[45]
DNA concatamers/gold surface	$[Ru(NH_3)_6]3^+$ based electrochemical sensing	Differential pulse voltammetry	HIV DNA	5 aM	Yes	[48]
DNA tetrahedron/gold surface	TMB-based electrochemical transduction	Cyclic voltammetry and amperometry	Whole cancer cells (aptamer of EpCAM)	4 cancer cells	Yes	[50]
DNA tetrahedron/gold surface	TMB-based electrochemical transduction	Amperometry	TNF-α	100 pg/mL	No	[53]
DNA nanoswitch (stem-loop)	Conformational change	Optical (FRET)	Specific mono- and bivalent proteins/antibodies	~5 nM	No	[55]

environments to ensure appropriate protein folding,[58] gas exchange,[59] enzyme function,[60] and cellular apoptosis.[61] For these reasons, developing biosensors capable of detecting and responding to pH changes have enormous implications for biomedical applications. In addition, cancer cells exhibit pH dysregulation and thus applications of pH sensors also extend to diagnostic purposes.[62]

Liu et al.[63] made one of the earliest DNA constructs that used the pH of the environment to induce a conformational change in an array of proton-fueled DNA motors and they reversibly actuated it by changing the solution pH between 4.5 and 9.0 (**Figure 5**a). They immobilized the motor onto a gold surface through a 5′ thiol modification. A fluorophore was attached to its 3′ end. In acidic conditions, the motor adopted a closed i-motif structure,[64] causing the distance between the termini to shorten, and the fluorophore to be quenched by the gold surface.[65] At basic conditions, the i-motif unraveled and the motor was able to bind with its complementary strand in solution, creating an elongated duplex. The fluorophore, being at least 2.5 nm pushed away from the gold surface, was able to fluoresce, demonstrating a type of fluorescence-based switch dependent on pH.

Modi et al.[66] constructed the first DNA nanomachine to function as a pH sensor inside living cells, based on an intramolecular i-motif called the I-switch. The basis of this machine was a conformational change from an open linear structure under physiological conditions (pH 7.3) to a closed triangular structure under acidic conditions (pH 5.0) (Figure 5b). Measurement of FRET between the fluorescent dyes attached to the 5′ and 3′ ends confirmed this conformational change.[67] The switch functioned as an efficient pH sensor with a pH range of 5.5 to 6.8. In a series of pulse and chase experiments, the I-switch was endocytosed into Drosophila hemocytes for mapping the spatial and temporal pH changes associated with endosome maturation. Transferrin, a protein of the β globulin group,[68] and the switch were biotinylated and then conjugated together using streptavidin to yield a transferrin-modified I-switch (Figure 5c) that was used to label a specific endocytic pathway. This device proved promising but with a timescale of 1–2 minutes and a pH range of 1.3 units, was limited in measuring biological pH changes on shorter timescales and broader pH ranges. Nonetheless, it demonstrated that DNA nanomachines could be used in living systems to measure real time pH changes in a crowded cellular environment.

A few years later the same group used this strategy to construct two distinct DNA nanomachines (Figure 5b,d) that could map simultaneously the pH gradients along two different but intersecting endocytic pathways inside the same cell.[69] The furin retrograde and transferrin receptor endocytic pathways were chosen, as these pathways merge in early endosomes before segregating into late endosomes and recycling endosomes, respectively.[70] Each device was programmed to have an appropriate pH response for the

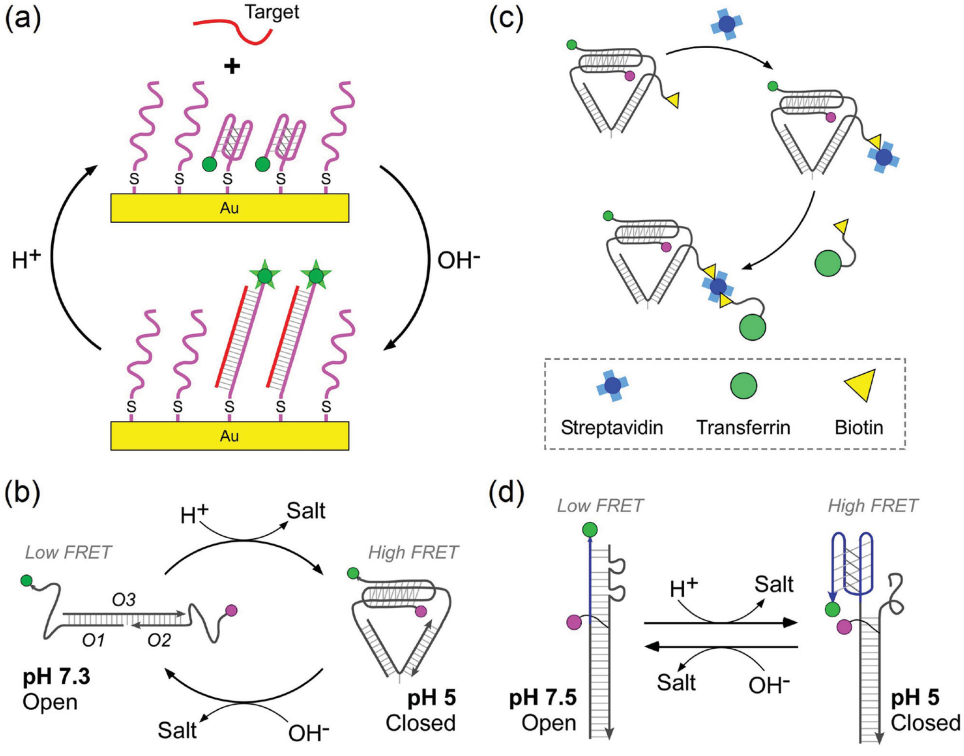

Figure 5. i-motif based pH sensors. a) Schematic of a reversible pH-driven DNA array: DNA probe adopts a closed i-motif structure at low pH (fluorescence quenched) and an open conformation at high pH moving the dye away from the surface on binding to its complementary strand (high fluorescence).[63] b) Conformational change from the 'open' state (high pH) to the 'closed' state (low pH) of the 'I-switch'.[66] c) A biotinylated transferrin was tagged to a biotinylated I-switch through streptavidin and used to label a specific endocytic pathway.[66] d) Another type of I-switch consisting of a duplex with a pH-responsive element that forms an intramolecular I-motif at low pH.[69] This leads to high FRET between the two dyes (green and pink).

organelles encountered as well as ideal FRET pairs for concurrent measurements without interference or cross-talk between the sensors. The two DNA nanomachines were optimized to work at pH levels 5.0–6.5 and 5.5–7.0 for the furin pathway and transferrin receptor pathway respectively. The DNA nanomachines were able to map simultaneously the spatiotemporal pH changes along the targeted pathways in distinct compartments and also in tandem within the same compartment to detect pH dynamics. Surana et al.[71] used this pH-triggered I-switch to map pH changes inside the nematode *Caenorhabditis elegans*. They used the switch to map, autonomously and effectively, the spatiotemporal pH changes associated with endocytosis in wild type as well as mutant worms. This was the first demonstration of the independent functionality of a DNA nanomachine in vivo.

The I-switch, while functional and ideal for monitoring intracellular pH changes, required costly and complicated synthetic steps to covalently label it to transferrin through biotin and streptavidin. Li et al.[72] improved this strategy by using graphene as a linker and cargo transporter. Graphene is a useful nanomaterial when used as graphene oxide (GO) as it has the ability to adsorb ssDNA, quench the fluorescence of a fluorophore, and serve as a molecular transporter of DNA into living cells while protecting the oligonucleotides from enzymatic degradation.[73] The construct used by Li et al.[72] was a simple duplex containing a 5-nucleotide hinge and a fluorescently labeled ssDNA overhang containing a triplex forming oligonucleotide (TFO) (**Figure 6**a). When protonated at acidic pH, the ssDNA overhang folds and binds to the duplex via Hoogsteen base pairing, thus forming a triplex. At basic pH, the switch displayed reversibility as the cytosine residues were deprotonated, causing the TFO to become unstable and dissociate, thus reforming the partial duplex. The fluorophore of the ssDNA domain was effectively quenched upon adsorption onto the GO sheet due to FRET between rhodamine green and GO. The quenching ability of the GO sheet was neutralized at acidic pH as the duplex transformed into a triplex, causing a release of the TFO from the surface of the GO sheet and allowing for fluorescence recovery.

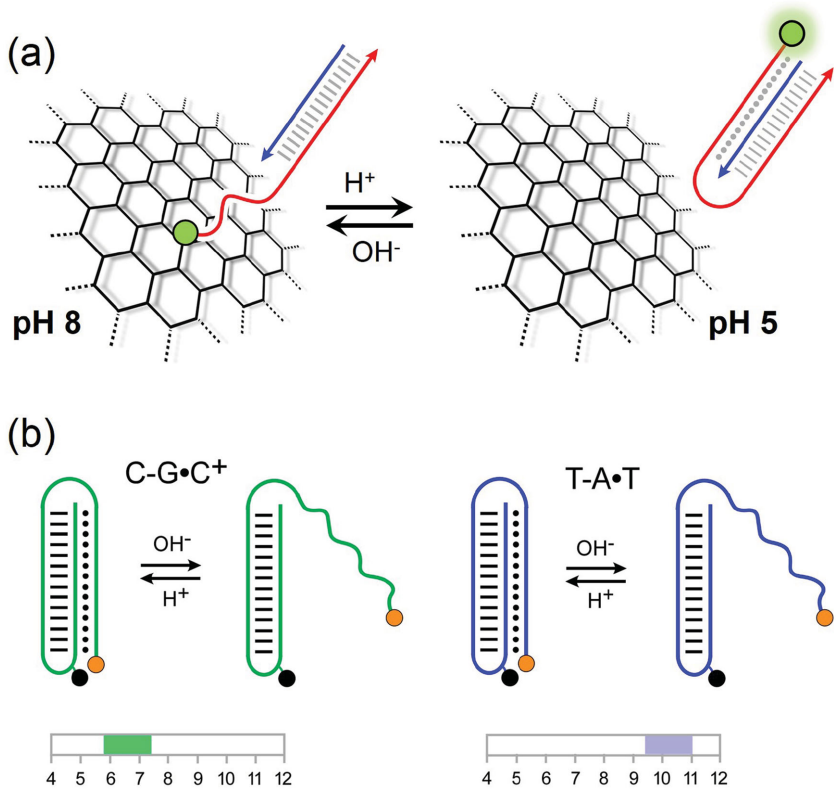

Figure 6. Triplex-based pH sensors. a) Schematic illustration of a graphene oxide-based pH sensor.[72] The single-stranded portion of the DNA complex tagged with a fluorescent dye is adsorbed onto the graphene oxide surface at high pH (quenched fluorescence, left). At low pH, the single-stranded extension folds back to form a triplex (high fluorescence, right). b) pH-triggered nanoswitches that form an intramolecular triplex structure.[74] The switches can be configured to contain varying amounts of T.AT triplets. Since a C^+.GC triplet requires acidic pH, switches containing only C^+.GC triplets open at pH levels 6.0–7.0 while those containing T.AT triplets open at pH levels 9.0–11.0. The pH sensitivity windows of the two switches are shown as a pH scale below the complexes.

To solve the problem of the narrow pH window and slow timescale typically seen in DNA-based pH sensor systems, Idili et al.[74] developed programmable DNA-based nanoswitches that could be modified to accommodate a range more than five units of pH with a response time in milliseconds (Figure 6b). Their switch took advantage of the fact that while Watson-Crick (WC) base pairing remains stable in acidic conditions, Hoogsteen interactions show a strong dependence on pH.[75] The switch formed a traditional WC duplex with a 10-nucleotide overhang that transitioned into a pH-triggered triplex due to parallel Hoogsteen interactions.[76] A pH-insensitive fluorophore attached to the 5′ end and a quencher internally positioned in the device, tracked the duplex to triplex transition. C^+.GC parallel triplets are destabilized at pH levels above 6.5 due to cytosine deprotonation, whereas T.AT triplets remain stable at physiological pH and only begin to dissociate at pH above 10 due to thymine deprotonation.[77] Altering the relative content of C^+.GC/T.AT triplets in the sequence modified the pH range of the switch. The transition of a switch with 100% T.AT triplets occurred at basic pH levels, 9.0–11.0 while the transition for a switch with 50% T.AT triplets occurred at a more acidic pH range, 5.0–7.0. Combining switches of different T.AT triplet content (50%, 80%, 100%) together created a pH sensor exhibiting a pH window of ~5.5 units. A similar strategy can also be used to trigger other dynamic strand displacement reactions using the TFO as a sensing motif.[78a] Moreover, similar motifs have been used to control Hybridization Chain Reactions (HCR) and might be useful for creating sensitive sensors that amplify signals based on pH changes.[78b] In addition, inclusion of pH sensitive domains in nanostructures allows us to trigger the

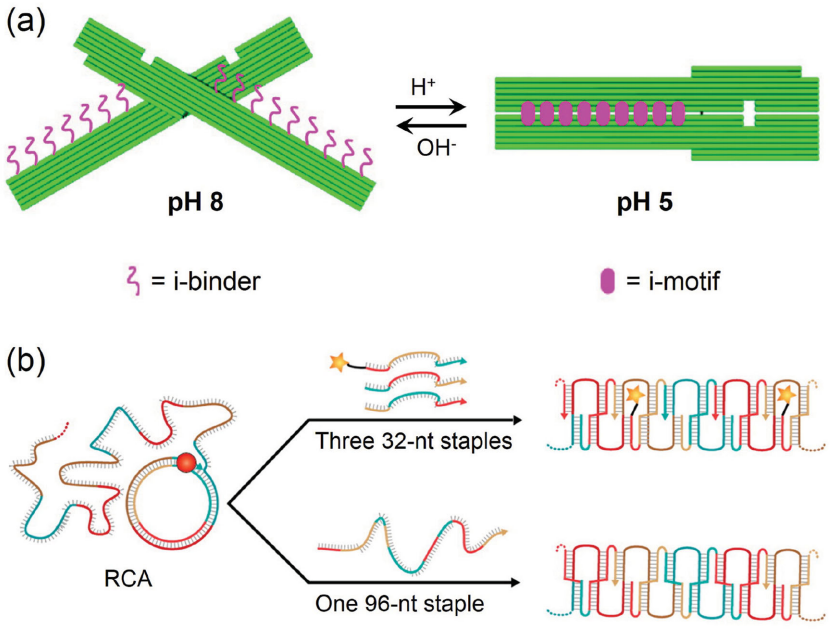

Figure 7. Origami-based pH sensors. a) Schematic of the DNA origami nanopliers: At high pH, the structure is in an open conformation. At low pH, the C-rich strands (i-binders) on each lever form an i-motif by binding to those on the other lever. Adapted with permission.[79] b) Schematic representation of the enzymatic synthesis of DNA nanoribbons using an RCA scaffold strand and three 32-nt staple strands (top) or one 96-nt staple strand (bottom). Carboxyfluorescein, a pH-sensitive dye, was attached to one of the staple strands and used to probe intracellular pH. Adapted with permission.[80] Copyright 2015, ACS.

delivery of specific target molecules.[78c] Such strategies provide dual functionality to biosensors: to both sense the target molecule and release the cargo in its presence.

Kuzuya et al.[79] have constructed a nanomechanical pH sensor using DNA origami. Their strategy involved pH-responsive shape transition of a DNA origami device and imaging using AFM (**Figure 7**a). These DNA origami 'pliers' were designed to contain C-rich sequences (i-binders) on each lever of the plier. Under acidic conditions, these sequences form an intermolecular i-motif thereby bringing the two levers together. This structural transition can be visualized using AFM. While DNA origami can be used to create such functional devices, it is often costly, involving hundreds of staple strands to manipulate a scaffold, and not practical for mass production. Chen et al.[80] made a periodic DNA nanoribbon from a modified DNA origami method that reduces the number of staple strands necessary to 3 or less (Figure 7b). They employed rolling circle amplification (RCA) to create long ssDNA with tandem repeats complementary to the circular template.[81] The RCA product was folded with 1 concatenated or 3 distinct staple strands to yield a 1-D periodic structure with high aspect ratio. Due to its unique structure and integrity, the DNA nanoribbons were able to internalize effectively into cells. One of the staple strands was labeled with a fluorescein derivative dye, carboxyfluorescein (FAM). FAM displays pH-dependent ratiometric fluorescence changes,[82] thus allowing the pH variations inside different regions of cells to be mapped. This DNA nanoribbon-FAM complex was able to exhibit desired intracellular pH response sensitivity in a crowded cellular milieu. **Table 3** summarizes the various DNA-based pH sensors discussed in this section.

5. Conclusion

Several DNA-based nanostructures have been constructed to respond to a variety of external chemical and biological stimuli. Such nanostructures provide a route to spatial arrangement of additional molecules via functionalization with a variety of ligands and chemical groups. These hybrid materials hold promise for versatile and sensitive molecular sensing that is not achievable using conventional sensing methods. In addition, the versatility of DNA-based nanostructures allows simultaneous detection of multiple targets with high sensitivity using a variety of amplification strategies. For example, the DNA tetrahedral structures discussed here have been modified for use with different types of targets. However, amplification of the output signals involves multiple steps. Solution-based or surface-based assays that involve minimal preparation methods would be easily accessible to more researchers for detection purposes. Also, DNA nanostructures have been shown to be robust for detection in cells and in vivo. The design and synthesis of these structures are specific to the particular host and generic

Table 3. Summary of pH sensing strategies.

Structure	Strategy	Read out	pH range	System	Reference
ssDNA/gold surface	Intramolecular i-motif formation	Fluorescence	4.5–9.0	In vitro	[63]
I-switch	Intramolecular i-motif formation	FRET/confocal	5.5–6.8	In cellulo	[66]
I-switch	Intramolecular i-motif formation	FRET/confocal	5.0–7.0	In cellulo	[69]
I-switch	Intramolecular i-motif formation	FRET/confocal	5.3–6.6	In vivo	[71]
Graphene oxide/triplex forming oligonucleotide	Intermolecular triplex formation	FRET	5.0–8.0	In cellulo	[72]
Double hairpin with triplex forming oligonucleotides	Intramolecular triplex formation	Fluorescence	5.5–11.0	In vitro	[74]
DNA origami nanopliers	Intermolecular i-motif formation	AFM	5.6–8.2	In vitro	[79]
DNA nanoribbons	pH-sensitive fluorescent dye	Confocal	4.0–8.0	In cellulo	[80]

design strategies would aid in the development of a wide variety of sensors. Future work on DNA-based chemical and biological sensors will especially aid in characterization and development of these structures for in situ sensing. DNA origami has made the construction of nanoscale objects easier and has widespread uses in biotechnology.[83] Moreover, the cost of synthetic DNA used for these purposes has been reduced in recent times,[84] and custom-made DNA origami scaffolds provide purpose-specific nanostructures.[85] One such advancement is the recently developed origami-based structures that provide an interface for presenting specifically patterned ligands to cells.[86] Origami-based structures allow the study of biomolecular interaction which can be incorporated into future sensor fabrication. Development of DNA nanostructure-based sensors will also help in understanding complex biological systems while providing a route to highly specific and sensitive detection.

[1] A. R. Chandrasekaran, J. Venugopal, S. Sundarrajan, S. Ramakrishna, *Biomed. Mater.* **2011**, *6*, 015001.
[2] S. Sundarrajan, A. R. Chandrasekaran, S. Ramakrishna, *J. Am. Ceram. Soc.* **2010**, *93*, 3955.
[3] a) N. C. Seeman, *Annu. Rev. Biochem.* **2010**, *79*, 65; b) A. R. Chandrasekaran, R. Zhuo, *Appl. Mater. Today* **2016**, *2*, 7; c) M. R. Jones, N. C. Seeman, C. A. Mirkin, *Science* **2015**, *347*, 1260901; d) A. R. Chandrasekaran, *Nanoscale* **2016**, *8*, 4436.
[4] a) E. Winfree, F. Liu, L. A. Wenzler, N. C. Seeman, *Nature* **1998**, *394*, 539; b) Y. He, Y. Tian, Y. Chen, Z. Deng, A. E. Ribbe, C. Mao, *Angew. Chem., Int. Ed.* **2005**, *44*, 6694; c) H. Yan, S. H. Park, G. Finkelstein, J. H. Reif, T. H. LaBean, *Science* **2003**, *301*, 1882.
[5] a) J. Zheng, J. J. Birktoft, Y. Chen, T. Wang, R. Sha, P. E. Constantinou, S. L. Ginell, C. Mao, N. C. Seeman, *Nature* **2009**, *461*, 74; b) R. Sha, J. J. Birktoft, N. Nguyen, A. R. Chandrasekaran, J. Zheng, X. Zhao, C. Mao, N. C. Seeman, *Nano Lett.* **2013**, *13*, 793; c) D. A. Rusling, A. R. Chandrasekaran, Y. P. Ohayon, T. Brown, K. R. Fox, R. Sha, C. Mao, N. C. Seeman, *Angew. Chem., Int. Ed.* **2014**, *53*, 3979; d) J. Zhao, A. R. Chandrasekaran, Q. Li, X. Li, R. Sha, N. C. Seeman, C. Mao, *Angew. Chem., Int. Ed.* **2015**, *54*, 9936.
[6] a) Y. P. Ohayon, R. Sha, O. Flint, A. R. Chandrasekaran, H. Abdallah, T. Wang, X. Wang, X. Zhang, N. C. Seeman, *ACS Nano* **2015**, *9*, 10296; b) Y. P. Ohayon, R. Sha, O. Flint, W. Liu, B. Chakraborty, H. K. K. Subramanian, J. Zheng, A. R. Chandrasekaran, H. Abdallah, X. Wang, X. Zhang, N. C. Seeman, *ACS Nano* **2015**, *9*, 10304.
[7] a) S. M. Douglas, I. Bachelet, G. M. Church, *Science* **2012**, *335*, 831; b) J. Bath, A. J. Turberfield, *Nat. Nanotechnol.* **2007**, *2*, 275.
[8] F. C. Simmel, W. U. Dittmer, *Small* **2005**, *1*, 284.
[9] a) M. T. Record Jr., S. J. Mazur, P. Melançon, J. H. Roe, S. L. Shaner, L. Unger, *Annu. Rev. Biochem.* **1981**, *50*, 997; b) P. K Mandal, A. R. Chandrasekaran, B. R. Madhanagopal, S. Venkadesh, N. Gautham, *J. Cryst. Growth* **2012**, *354*, 20; c) D. Svozil, J. Kalina, M. Omelka, B. Schneider, *Nucleic Acids Res.* **2008**, *36*, 3690.
[10] C. Mao, W. Sun, Z. Shen, N.C. Seeman, *Nature* **1999**, *397*, 144.
[11] a) J. D. Slinker, N. B. Muren, S. E. Renfrew, J. K. Barton, *Nat. Chem.* **2011**, *3*, 228; b) J. C. Genereux, J. K. Barton, *Chem. Rev.* **2010**, *110*, 1642.
[12] a) L. Qian, E. Winfree, J. Bruck, *Nature* **2011**, *475*, 368; b) R. J. Pei, E. Matamoros, M. H. Liu, D. Stefanovic, M. N. Stojanovic, *Nat. Nanotechnol.* **2010**, *5*, 773.
[13] D. Bhatia, S. Surana, S. Chakraborty, S. P. Koushika, Y. Krishnan, *Nat. Commun.* **2011**, *2*, 339.
[14] a) J. Li, H. Pei, B. Zhu, L. Liang, M. Wei, Y. He, N. Chen, D. Li, Q. Huang, C. *ACS Nano* **2011**, *5*, 8783; b) H. Lee, A. K. R. Lytton-Jean, Y. Chen, K. T. Love, A. I. Park, E. D. Karagiannis, A. Sehgal, W. Querbes, C. S. Zurenko, M. Jayaraman, C. G. Peng, K. Charisse, A. Borodovsky, M. Manoharan, J. S. Donahoe, J. Truelove, M. Nahrendorf, R. Langer, D. G. Anderson, *Nat. Nanotechnol.* **2012**, *7*, 389; c) A. R. Chandrasekaran, N. Anderson, M. Kizer, K. Halvorsen, X. Wang, *ChemBioChem* **2016**, DOI: 10.1002/cbic.201600038.
[15] D. Luo, *Mater. Today* **2003**, *6*, 38.
[16] U. Feldkamp, C. M. Niemeyer, *Angew. Chem., Int. Ed.* **2006**, *45*, 1856.
[17] M. Schena, D. Shalon, R. W. Davis, P. O. Brown, *Science* **1995**, *270*, 467.
[18] S. A Bustin, T. Nolan, *J. Biomol. Tech.* **2004**, *15*, 155.
[19] a) J. Shendure, H. Ji, *Nat. Biotechnol.* **2008**, *26*, 1135; b) C. Meldrum, M. A. Doyle, R. W. Tothill, *Clin. Biochem. Rev.* **2011**, *32*, 177.
[20] Y. H. Yang, T. Speed, *Nat. Rev. Genet.* **2002**, *3*, 579.
[21] D. Gerion, F. Chen, B. Kannan, A. Fu, W. J. Parak, D. J. Chen, A. Majumdar, A. Paul Alivisatos, *Anal. Chem.* **2003**, *75*, 4766.
[22] Q. Guo, X. Yang, K. Wang, W. Tan, W. Li, H. Tang, H. Li, *Nucleic Acids Res.* **2009**, *37*, e20.
[23] C. M. Erben, R. P. Goodman, A. J. Turberfield, *Angew. Chem., Int. Ed.* **2006**, *45*, 7414.
[24] H. Pei, N. Lu, Y. Wen, S. Song, Y. Liu, H. Yan, C. Fan, *Adv Mater.* **2010**, *22*, 4754.
[25] a) M. J. Heller, *Annu. Rev. Biomed. Eng.* **2002**, *4*, 129; b) E. L. S. Wong, E. Chow, J. J. Gooding, *Langmuir* **2005**, *21*, 6957.
[26] C. Fan, K. W. Plaxco, A. J. Heeger, *Proc. Natl. Acad. Sci. USA* **2003**, *100*, 9134.
[27] G. Liu, Y. Wan, V. Gau, J. Zhang, L. Wang, S. Song, C. Fan, *J. Am. Chem. Soc.* **2008**, *130*, 6820.
[28] M. Lin, J. Wang, G. Zhou, J. Wang, N. Wu, J. Lu, J. Gao, X. Chen, J. Shi, X. Zuo, C. Fan, *Angew. Chem., Int. Ed.* **2015**, *54*, 2151.
[29] a) F. Ricci, N. Zari, F. Caprio, S. Recine, A. Amine, D. Moscone, G. Palleschi, K. W. Plaxco, *Bioelectrochemistry* **2009**, *76*, 208; b) L. Soleymani, Z. C. Fang, E. H. Sargent, S. O. Kelley, *Nat. Nanotechnol.* **2009**, *4*, 844.
[30] a) K. Halvorsen, D. Schaak, W. P. Wong, *Nanotechnology* **2011**, *22*, 494005; b) M. A. Koussa, K. Halvorsen, A. Ward, W. P. Wong, *Nat. Methods* **2015**, *12*, 123.
[31] A. R. Chandrasekaran, J. Zavala, K. Halvorsen, *ACS Sens.* **2016**, *1*, 120.
[32] P. Lie, J. Liu, Z. Fang, B. Dun, L. Zeng, *Chem. Commun.* **2012**, *48*, 236.
[33] P. W. K. Rothemund, *Nature* **2006**, *440*, 297.
[34] Y. Ke, S. Lindsay, Y. Chang, Y. Liu, H. Yan, *Science* **2008**, *319*, 180.
[35] a) F. S. Collins, L. D. Brooks, A. Chakravarti, *Genome Res.* **1998**, *8*, 1229; b) F. S. Collins, M. Morgan, A. Patrinos, *Science* **2003**, *300*, 286.
[36] a) J. R. Vieregg, H. M. Nelson, B. M. Stoltz, N. A. Pierce, *J. Am. Chem. Soc.* **2013**, *135*, 9691; b) J. S. Wang, D. Y. Zhang. *Nat. Chem.* **2015**, *7*, 545.
[37] S. X. Chen, D. Y. Zhang, G. Seelig. *Nat. Chem.* **2013**, *5*, 782.
[38] Z. Zhang, D. Zeng, H. Ma, G. Feng, J. Hu, L. He, C. Li, C. Fan, *Small* **2010**, *6*, 1854.
[39] Z. Zhang, Y. Wang, C. Fan, C. Li, Y. Li, L. Qian, Y. Fu, Y. Shi, J. Hu, L. He, *Adv. Mater.* **2010**, *22*, 2672.
[40] B. Yurke, A. J. Turberfield, A. P. Mills Jr., F. C. Simmel, J. L. Neumann, *Nature* **2000**, *406*, 605.
[41] I. G. Panyutin, P. Hsieh, *Proc. Natl. Acad. Sci. USA* **1994**, *91*, 2021.
[42] H. K. K. Subramanian, B. Chakraborty, R. Sha, N. C. Seeman, *Nano Lett.* **2011**, *11*, 910.
[43] D. A. Giljohann, C. A. Mirkin, *Nature* **2009**, *462*, 461.
[44] a) D. Li, S. Song, C. Fan, *Acc. Chem. Res.* **2010**, *43*, 631; b) F. Wang, J. Elbaz, R. Orbach, N. Magen, I. Willner, *J. Am. Chem. Soc.* **2011**, *133*, 17149.
[45] Y. Li, Y. T. H. Cu, D. Luo, *Nat. Biotechnol.* **2005**, *23*, 885.

[46] Y. Li, Y. D. Tseng, S. Y. Kwon, L. d'Espaux, J. S. Bunch, P. L. McEuen, D. Luo, *Nat. Mater.* **2004**, *3*, 38.
[47] a) Y. Zhang, Y. Wang, H. Wang, J. H. Jiang, G. L. Shen, R. Q. Yu, J. Li, *Anal. Chem.* **2009**, *81*, 1982; b) Y. Xiao, X. Lou, T. Uzawa, K. J. I. Plakos, K. W. Plaxco, T. Soh, *J. Am. Chem. Soc.* **2009**, *131*, 15311; c) Y. Peng, Z. Gao, *Anal. Chem.* **2011**, *83*, 820.
[48] X. Chen, C. Y. Hong, Y. H. Lin, J. H. Chen, G. N. Chen, H. H. Yang, *Anal. Chem.* **2012**, *84*, 8277.
[49] a) H. J. Yoon, T. H. Kim, Z. Zhang, E. Azizi, T. M. Pham, C. Paoletti, J. Lin, N. Ramnath, M. S. Wicha, D. F. Hayes, D. M. Simeone, S. Nagrath, *Nat. Nanotechnol.* **2013**, *8*, 735; b) S. C. P. Williams, *Proc. Natl. Acad. Sci. USA* **2013**, *110*, 4861; c) V. Plaks, C. D. Koopman, Z. Werb, *Science* **2013**, *341*, 1186.
[50] G. Zhou, M. Lin, P. Song, X. Chen, J. Chao, L. Wang, Q. Huang, W. Huang, C. Fan, X. Zuo, *Anal. Chem.* **2014**, *86*, 7843.
[51] W. Zhao, C. H. Cui, S. Bose, D. Guo, C. Shen, W. P. Wong, K. Halvorsen, O. C. Farokhzad, G. S. L. Teo, J. A. Philips, D. M. Dorfman, R. Karnik, J. M. Karp, *Proc. Natl. Acad. Sci. USA* **2012**, *109*, 19626.
[52] a) P. Paterlini-Brechot, N.L. Benali, *Cancer Lett.* **2007**, *253*, 180; b) C. Alix-Panabieres, K. Pantel, *Clin. Chem.* **2013**, *59*, 110.
[53] H. Pei, Y. Wan, J. Li, H. Hu, Y. Su, Q. Huang, C. Fan, *Chem. Commun.* **2011**, *47*, 6254.
[54] C.M. Niemeyer, *Angew. Chem., Int. Ed.* **2010**, *49*, 1200.
[55] S. Ranallo, M. Rossetti, K. W. Plaxco, A. Vallée-Bélisle, F. Ricci, *Angew. Chem., Int. Ed.* **2015**, *54*, 13214.
[56] a) S. Tyagi, F. R. Kramer, *Nat. Biotechnol.* **1996**, *14*, 303; b) S. A. E. Marras, S. Tyagi, F. R. Kramer, *Clin. Chim. Acta* **2006**, *363*, 48.
[57] H. E. Androgue, H. J. Androgue, *Respiratory Care* **2001**, *46*, 328.
[58] a) K. A. Dill, *Biochemistry* **1990**, *29*, 7133; b) C. M. Dobson, *Nature* **2003**, *426*, 884.
[59] A. Bidani, E. D. Crandall, R. E. Forster, *J. Appl. Physiol.* **1978**, *44*, 770.
[60] B. Trivedi, W. H. Danforth, *J. Biol. Chem.* **1966**, *241*, 4110.
[61] a) D. Lagadic-Gossmann, L. Huc, V. Lecureur, *Cell Death Differ.* **2004**, *11*, 953; b) S. Matsuyama, J. C. Reed, *Cell Death Differ.* **2000**, *7*, 1155.
[62] B. A. Webb, M. Chimenti, M. P. Jacobson, D. L. Barber, *Nat. Rev.* **2011**, *11*, 671.
[63] D. Liu, A. Bruckbauer, C. Abell, S. Balasubramanian, D. J. Kang, D. Klenerman, D. Zhou, *J. Am. Chem. Soc.* **2006**, *128*, 2067.
[64] K. Gehring, J. L. Leroy, M. Gueron, *Nature* **1993**, *363*, 561.
[65] B. Duberrtret, M. Calame, A. Libchaber, *Nat. Biotechnol.* **2001**, *19*, 365.
[66] S. Modi, M. G. Swetha, D. Goswami, G. D. Gupta, S. Mayor, Y. Krishnan, *Nat. Nanotechnol.* **2009**, *4*, 325.
[67] L. Stryer, R. P. Haugland, *Proc. Natl Acad. Sci. USA* **1967**, *58*, 719.
[68] D. M. Sipe, R. F. Murphy, *Proc. Natl Acad. Sci. USA* **1987**, *84*, 7119.
[69] S. Modi, C. Nizak, S. Surana, S. Halder, Y. Krishnan, *Nat. Nanotechnol.* **2013**, *8*, 459.
[70] a) W. G. Mallet, F. R. Maxfield, *J. Cell. Biol.* **1999**, *146*, 345; b) P. Z. C. Chia, I. Gasnereau, Z. Z. Lieu, P. A. Gleeson, *J. Cell. Sci.* **2011**, *124*, 2401.
[71] S. Surana, J. M. Bhat, S. P. Koushika, Y. Krishnan. *Nat. Commun.* **2011**, *2*, 340.
[72] X. M. Li, J. Song, T. Cheng, P. Y. Fu, *Anal. Bioanal. Chem.* **2013**, *405*, 5993.
[73] a) Y. Wang, Z. Li, D. Hu, C. T. Lin, J. Li, Y. Lin, *J. Am. Chem. Soc.* **2010**, *132*, 9274; b) C. H. Lu, H. H. Yang, C. L. Zhu, X. Chen, G. N. Chen, *Angew. Chem., Int. Ed.* **2009**, *48*, 4785; c) X. H. Zhao, R. M. Kong, X. B. Zhang, H. M. Meng, W. N. Liu, W. H. Tan, G. L. Shen, R. Q. Yu, *Anal. Chem.* **2011**, *83*, 5062.
[74] A. Idili, A. Vallee-Belisle, F. Ricci, *J. Am. Chem. Soc.* **2014**, *136*, 5836.
[75] a) T. Ohmichi, Y. Kawamoto, P. Wu, D. Miyoshi, H. Karimata, N. Sugimoto, *Biochemistry* **2005**, *44*, 7125; b) D. Leitner, W. Schoder, K. Weisz, *Biochemistry* **2000**, *39*, 5886; c) N. Sugimoto, P. Wu, H. Hara, Y. Kawamoto, *Biochemistry* **2001**, *40*, 9396.
[76] V. Sklena, J. Felgon, *Nature* **1990**, *345*, 836.
[77] a) J. L. Asensio, A. N. Lane, J. Dhesi, S. Berggvist, T. Brown, *J. Mol. Biol.* **1998**, *275*, 811; b) A. M. Soto, J. Loo, L. A. Marky, *J. Am. Chem. Soc.* **2002**, *124*, 14355.
[78] a) A. Amodio, B. Zhao, A. Porchetta, A. Idili, M. Castronovo, C. Fan, F. Ricci. *J. Am. Chem. Soc.* **2014**, *136*, 16469; b) A. Idili, A. Porchetta, A. Amodio, A. Vallée-Bélisle, F. Ricci, *Nano Lett.* **2015**, *15*, 5539; c) A. Porchetta, A. Idili, A. Vallée-Bélisle, F. Ricci, *Nano Lett.* **2015**, *15*, 4467.
[79] A. Kuzuya, R. Watanabe, Y. Yamanaka, T. Tamaki, M. Kaino, Y. Ohya, *Sensors* **2014**, *14*, 19329.
[80] G. Chen, D. Liu, C. He, T. R. Gannett, W. Lin, Y. Weizmann, *J. Am. Chem. Soc.* **2015**, *137*, 3844.
[81] Y. Ma, H. Zheng, C. Wang, Q. Yan, J. Chao, C. Fan, S. J. Xiao, *J. Am. Chem. Soc.* **2013**, *135*, 2959.
[82] C. He, K. Lu, W. Lin, *J. Am. Chem. Soc.* **2014**, *136*, 12253.
[83] A. R. Chandrasekaran, *J. Chem. Technol. Biotechnol.* **2016**, *91*, 843.
[84] A. N. Marchi, I. Saaem, B. N. Vogen, S. Brown, T. H. LaBean, *Nano Lett.* **2014**, *14*, 5740.
[85] A. R. Chandrasekaran, M. Pushpanathan, K. Halvorsen, *Mater. Lett.* **2016**, *170*, 221.
[86] A. Angelin, S. Weigel, R. Garrecht, R. Meyer, J. Bauer, R. K. Kumar, M. Hirtz, C. M. Niemeyer, *Angew. Chem,. Int. Ed.* **2015**, *54*, 15813.

Received: December 19, 2015
Revised: January 23, 2016
Published online: April 4, 2016